

is set to be 20 Mbps. At each rising edge of the input data V_{in} , a UWB pulse is generated. As a result, a UWB pulse is transmitted for each data bit. The voltage swing of the pulse is around 600 mVp-p, and the pulse width is around 0.5 ns. The pulse repetition rate can be changed by varying the input clock rate because each pulse is generated by each rising edge of the clock. High-bit rate (50 Mbps) performance is also measured, as shown in Figure 6(b).

Figure 7 shows a measured spectrum of the DA output pulse sequence, where the data transmission rate is 50 Mbps. It can be seen that the pulse spectrum are shaped such that the major energy occupies in the FCC UWB low-band of 3.1–5 GHz and the power spectrum density is less than -41.3 dBm/MHz. The proposed UWB transmitter IC can also be used for other data rate. The measured transmitter IC performance is summarized in Table 2.

The antenna prototype is shown in Figure 8. The proposed monopole antenna is simulated and optimized using the commercial simulation software CST Microwave Studio simulator. Figure 9 shows return loss of the proposed antenna with a notched frequency band centered at 5.55 GHz.

The measured antenna radiation patterns at 4 and 7 GHz are plotted in Figure 10. At the low frequency, E-plane radiation pattern is similar to that of the traditional monopole antenna. For the H-plane radiation patterns, it is still remain nearly omnidirectional across the operation bandwidth. Although the proposed TX generates pulses that are below 5.1 GHz, the band-notch feature is still very helpful for next-generation UWB transceivers working at higher frequency range where the interference with WLAN at the band of 5.1–5.8 GHz has to be excluded by the design itself.

The received pulse signal transmitted by the UWB transmit module is shown in Figure 11. The measured pulse transmission result clearly demonstrated the workability of the proposed UWB transmit module.

5. CONCLUSION

A fully integrated CMOS UWB transmitter module is presented. The transmitter module consists of a band-notched UWB antenna and a transmitter IC which integrates a pulse generator, a gating signal generator and DAs. The UWB pulse generator proposed is all-digital, low-complexity and has low-power consumption. The drive amplifier uses a two-stage amplifier—a Class-E amplifier and a Class-A amplifier with switch control, to significantly reduce power consumption. The transmitter has been demonstrated in a $0.18\text{-}\mu\text{m}$ CMOS technology.

REFERENCES

1. I. Oppermann, H. Matti, and J. Iinatti, UWB theory and applications, John Wiley, 2004, Hoboken, NJ pp. 1–7.
2. L. Smaini, et al., Single-chip CMOS pulse generator for UWB systems, IEEE J Solid-State Circuits 41 (2006), 1551–1561.
3. D.D. Wentzloff and A.P. Chandrakasan, A 47pJ/pulse 3.1-to-5GHz All-Digital UWB Transmitter in 90 nm CMOS, In: IEEE international solid-state circuits conference (ISSCC), San Francisco, 2007, pp. 118–119
4. J. Ryckaert, et al., A 0.65-to-1.4nJ/burst 3-to-10GHz UWB Digital TX in 90nm CMOS for IEEE 802.15.4a, In: IEEE international solid-state circuits conference, San Francisco, 2007, pp. 120–591
5. Y. Zheng, et al., A CMOS carrier-less UWB transceiver for WPAN applications, In: IEEE international solid-state circuits conference (ISSCC), San Francisco, 2006, pp. 116–117.
6. H. Kim, D. Park, and Y. Joo, All-digital low-power CMOS pulse generator for UWB system, Electron Lett 40 (2004), 1534–1535.
7. T. Norimatsu, et al., A novel UWB impulse-radio transmitter with all-digitally-controlled pulse generator, In: Proceedings of ESSCIRC, Grenoble, France, 2006, pp. 267–270.
8. J. Ryckaert, et al., Ultra-wide-band transmitter for low-power wireless

body area networks: Design and evaluation, IEEE Trans Circuits Syst 52 (2005), 2515–2525.

9. H. Kim and Y. Joo, Fifth-derivative Gaussian pulse generator for UWB system, In: Proceedings of 2005 IEEE radio frequency integrated circuits (RFIC) symposium, Long Beach, CA, 2005, pp. 671–674.
10. S.W. Su, K.L. Wong, and C.L. Tang, Band-notched ultra-wideband planar-monopole antenna, Microwave Opt Technol Lett 44 (2005), 217–219.
11. J. Qiu, Z. Du, J. Lu, and K. Gong, A band-notched UWB antenna, Microwave Opt Technol Lett 45 (2005), 152–154.
12. C.W. Qiu, S. Zouhdi, and A. Razek, Modified spherical wave functions with anisotropy ratio: Application to the analysis of scattering by multilayered anisotropic shells, IEEE Trans Antennas Propag 55 (2007), 3515–3523.
13. Q.Q. Pei, C.W. Qiu, T. Yuan, and S. Zouhdi, Hybrid shaped ultra-wideband antenna, Microwave Opt Technol Lett 49 (2007), 2412–2415.
14. A. Bevilacqua and A.M. Niknejad, An ultra-wideband CMOS low-noise amplifier for 3.1-10.6 GHz wireless receivers, IEEE J Solid-State Circuits 39 (2004), 2259–2268.
15. K. Marsden, H.J. Lee, D.S. Ha, and H.S. Lee, Low power CMOS reprogrammable pulse generator for UWB systems, In: IEEE conference on ultra wideband systems and technologies, Reston, VA, 2003, pp. 443–447.

© 2009 Wiley Periodicals, Inc.

A HIGHLY EFFICIENT CLASS-F POWER AMPLIFIER FOR WIDEBAND LINEAR POWER AMPLIFIER APPLICATIONS

Jangheon Kim,¹ Junghwan Moon,¹ Sungchul Hong,² and Bumman Kim¹

¹ Department of Electrical Engineering, Pohang University of Science and Technology, Gyeongbuk 790-784, Republic of Korea; Corresponding author: rage3k@postech.ac.kr

² Telecommunication Research and Development Center, Samsung Electronics Company Ltd., Suwon, Gyeonggi 442-742, Republic of Korea

Received 22 January 2009

ABSTRACT: In this letter, a highly efficient class-F power amplifier (PA) is developed as a new main block of the wideband base-station linear power amplifier. The class-F PA is implemented using Eudyna EGN010MK GaN HEMT with a 10-W peak envelop power. The nonlinearity and memory effects of class-F PA are explored to apply the wide-band application. The maximum power-added efficiency of the implemented PA is 68% at a saturated output power of 40 dBm for the 2.14-GHz CW signal. The PA delivers a good efficiency of 35% at an average output power of 32.3 dBm for wide-band code division multiple access 3FA signal with 15-MHz bandwidth, and the linearity can be improved to about -48 dBc using the digital feedback predistortion linearization technique. © 2009 Wiley Periodicals, Inc. Microwave Opt Technol Lett 51: 2323–2326, 2009; Published online in Wiley InterScience (www.interscience.wiley.com). DOI 10.1002/mop.24631

Key words: power amplifier; efficiency; linearity; linearization; WC-DMA

1. INTRODUCTION

Current and next-generation wireless communication systems, such as wide-band code division multiple access (WCDMA), worldwide interoperability for microwave access (WiMAX) and so on, are progressed toward the wide band-width and large number of carriers to transmit high-data-rate signals for multime-

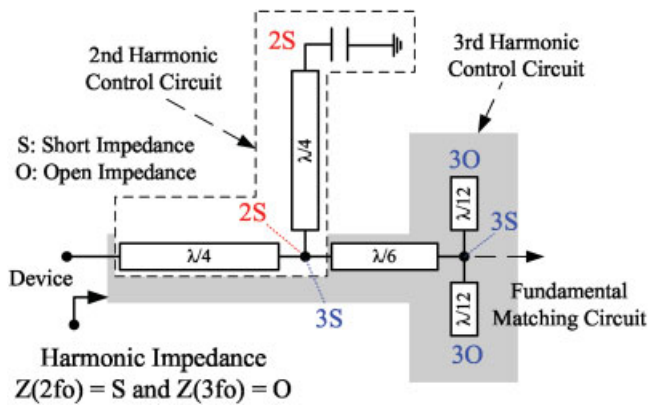


Figure 1 Harmonic control circuit of the class-F power amplifier. [Color figure can be viewed in the online issue, which is available at www.interscience.wiley.com]

dia communications. To sustain these communications, the power amplifiers (PAs) should amplify the modulated signals without distortion. However, the PAs cannot linearly amplify the signals due to severe memory effects for the wideband signals. Thus, the memory-effect suppression is an important issue for the applications. Moreover, a highly efficient PA is required to reduce size and cost of the overall system.

Recently, to accomplish the requirements of PAs, the switching/saturated PAs that are used as a main PA of a linear power amplifier (LPA) have been developed as well as other transmitter architectures using them [1–5]. This new scheme is based on the high efficiency performance of the PAs, and the linearity of the PAs mainly depends on the linearization capability of a digital predistortion (DPD) technique. Thus, the powerful DPD technique is required to compensate nonstandard or serious nonlinear characteristics of the PAs operated at the average power level.

This letter presents the highly efficient class-F PA that is used as a main PA of a LPA for WCDMA multi-carrier applications. The class-F PA is implemented using Eudyna EGN010MK GaN HEMT with a 10-W peak envelop power (PEP). The memory effects of the class-F PA are at first explored using two-tone signals (up to 20-MHz tone spacing). The digital feedback predistortion (DFBPD) technique that deliver a good linearization performance for serious nonlinear distortions due to the accurate predistortion (PD) signal extraction capability is applied to linearize the PA [6]. From the experimental results, it will be demonstrated that the implemented class-F PA delivers high efficiency and linearity performance for WCDMA 3FA signal with 15-MHz band-width.

2. CLASS-F PA DESIGN AND ANALYSIS

2.1. Circuit Topology

A class-F PA can achieve high efficiency by generating ideally half-sinusoidal current and square-wave voltage waveforms. These waveforms are realized by creating zero impedance at all even harmonics and infinite impedance at all odd harmonics. However, because all harmonic contents cannot be controlled, the class-F PA is mostly designed through the second and third harmonic controls. Figure 1 shows the harmonic control circuit (HCC) of the class-F PA. The control circuit is designed to provide a short impedance for the control harmonic frequency at cross-section point to prevent disturbances caused by other harmonic frequencies at the point. The harmonic control impedances should to be provided at the drain current node inside of the intrinsic capacitive components

and the packaging elements. Thus, a phase delay of the components and the packaging elements are compensated by reducing the length of the $\lambda/4$ line that is placed at the input of the HCC. In addition, the HCC is employed in front of the fundamental matching circuit to prevent the harmonic impedance change caused by the matching circuit as presented in [Ref. 7].

2.2. Memory-Effect Suppression

For the wideband signals, the memory effects are mainly caused by varying envelope and second harmonic node impedances according to the different modulated frequencies [8]. The impedances at the gate and drain nodes of the class-F PA can be expressed as

and

$$Z_{\text{Drain}}(f_2 - f_1, 2f_{1,2}) = Z_{\text{D,device}} // Z_{\text{D,HCC}} \quad (2)$$

To minimize the memory effects, the impedances should be zero or constant values for varying the frequency range. The short impedance at the gate node can be fulfilled by properly designing the bias circuit due to high input impedance $Z_{\text{G,device}}$. The second harmonic impedances at the drain node can be shorted right by the second harmonic control circuit of the class-F PA. Moreover, in the class-F PA design using a GaN HEMT device, the output load impedance $Z_{\text{D,device}}$ is increased due to the high power capacity of the device. Thus, it is possible to close a short envelope impedance through the HCC. Therefore, the memory effects of the class-F PA can be suppressed.

3. IMPLEMENTATION AND EXPERIMENTAL RESULTS

The class-F PA is implemented using Eudyna EGN010MK GaN HEMT with a 10-W peak envelop power (PEP) and has a class-B bias ($V_{\text{GG}} = -1.6$ V at $V_{\text{DD}} = 50$ V). Figure 2 shows the measured output power, power gain, drain efficiency, and power-added efficiency (PAE) of the class-F PA for a 2.14-GHz CW signal. The maximum PAE is 68% at a saturated output power of 40 dBm. Figure 3 illustrates the IMD3 and IMD5 characteristics of the PA for two-tone signals (up to 20-MHz tone spacing). The amplifier has serious nonlinear distortions at the whole output power range but has very weak memory effects for all average power levels and tone spacings. These characteristics are induced by the saturated

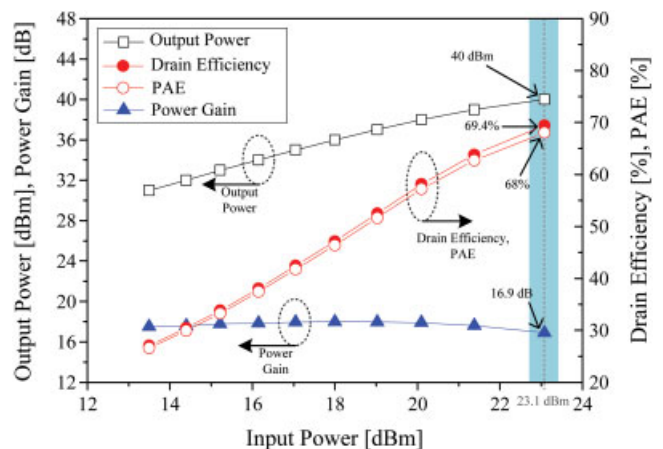


Figure 2 Measured output power, power gain, drain efficiency, and PAE characteristics for CW signal. [Color figure can be viewed in the online issue, which is available at www.interscience.wiley.com]

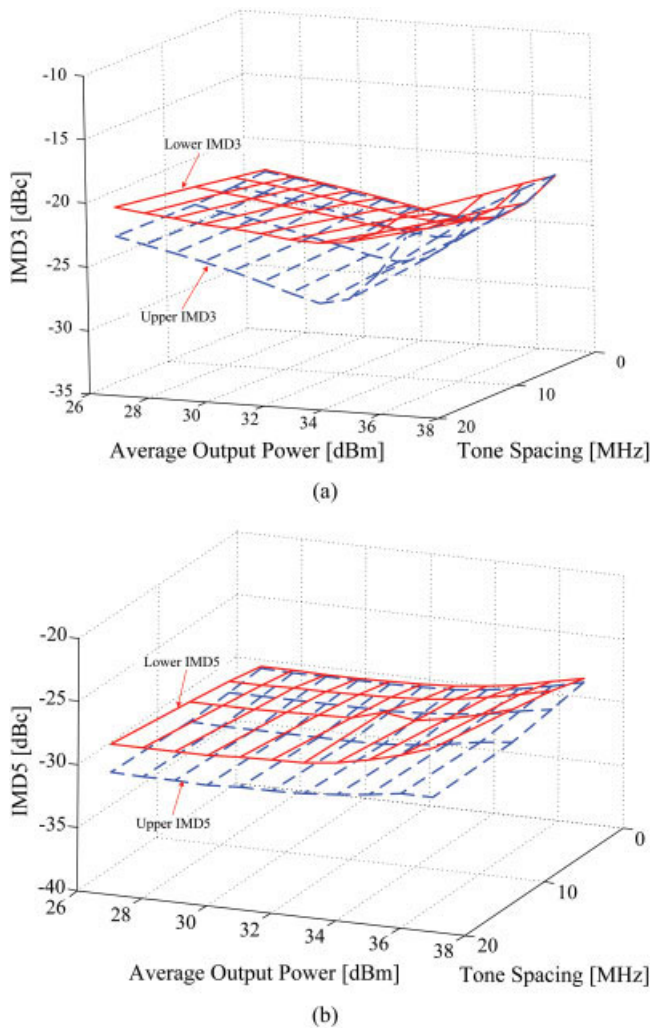


Figure 3 Measured (a) IMD3 and (b) IMD5 characteristics for two-tone signals (up to 20 MHz tone spacing). [Color figure can be viewed in the online issue, which is available at www.interscience.wiley.com]

operation to accomplish high efficiency and the low memory characteristics of class-F circuit topology using the GaN HEMT device, as expected in Section 2.

To verify the suitability of the class-F PA as the main block of the wideband base-station LPA, we have employed the DFBPD linearization technique to improve the linearity for a 2.14-GHz forward-link WCDMA 3FA signal with 15 MHz bandwidth and 8.2 dB peak-to-average power ratio (PAPR) at the 0.01% level of the complementary cumulative distribution function (CCDF). An Agilent Advanced Design System using an electronic signal generator and vector signal analyzer (ADS-ESG-VSA) connected solution was used for the test [9]. The DFBPD consists of two 256-entry AM/AM and AM/PM lookup tables (LUTs) which is programmed by MATLAB. Figure 4 illustrates AM/AM and AM/PM characteristics of the amplifier before the linearization at an average output power of 32.3 dBm. It is shown that the PA provides serious nonlinear characteristics at the whole input voltage range and has weak memory effects. These data indicate that it is important to linearize the serious nonlinear characteristics of the class-F PA, more than the memory-effect compensation.

Figure 5 shows the measured WCDMA 3FA spectra of the PA before and after the DFBPD linearization. The ACLR at an offset of 5-MHz is -48.2 dBc, which is an improvement of about 24 dB

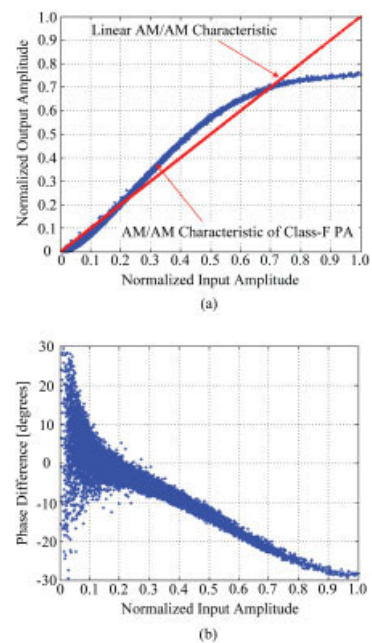


Figure 4 Measured (a) AM/AM and (b) AM/PM characteristics before the linearization at an average output power of 32.3 dBm for WCDMA 3FA signal. [Color figure can be viewed in the online issue, which is available at www.interscience.wiley.com]

at an average output power of 32.3 dBm. The PAE of the PA is 35% at the average output power. Figure 6 illustrates the AM/AM and AM/PM characteristics of the PA after the linearization. The serious memoryless nonlinear characteristics are successfully linearized by the DFBPD algorithm. In addition, to explore the better linearization possibility for the weak memory effects, the wideband digital feedback predistortion (WDFBPD) technique including a memory-effect compensation algorithm presented in [Ref. 10] is applied, and the linearization result is almost the same in comparison to the memoryless DFBPD linearization. These results show clearly that the class-F PA has weak memory effects and can deliver high efficiency as well as high linearity by employing the

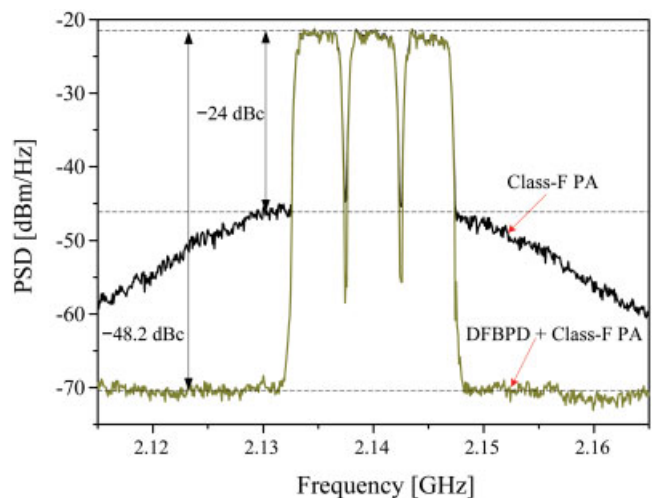


Figure 5 Measured WCDMA 3FA spectra before and after the DFBPD linearization at an average output power of 32.3 dBm. [Color figure can be viewed in the online issue, which is available at www.interscience.wiley.com]

memoryless DPD linearization for wideband signals. The measurement results are summarized in Table 1.

4. CONCLUSIONS

In this letter, the highly efficient class-F PA is presented as a new main block of the wideband base-station LPA. The nonlinearity and memory effects of class-F PA are investigated using the two-tone and modulated signals. The PA delivers a good efficiency of 35% at an average output power of 32.3 dBm for WCDMA 3FA signal with 15-MHz bandwidth, and the linearity can be improved to about -48 dBc using the DFBDP technique. From the experimental results, we conclude that the class-F PA is well suitable to the highly efficient main amplifier of the current and next-generation systems.

ACKNOWLEDGMENT

This work was supported by WCU (World Class University) program through the Korea Science and Engineering Foundation

TABLE 1 Measured Performance of the Class-F Amplifier Before and After the Linearization at an Average Output Power of 32.3 dBm (PAE = 35.0%) for WCDMA 3FA Signal

	ACLR [dBc] at ± 5 MHz	ACLR [dBc] at ± 10 MHz
Class-F PA	$-24.0/-25.4$	$-27.1/-28.9$
DFBDP + Class-F PA	$-48.2/-48.7$	$-48.3/-49.2$

funded by the Ministry of Education, Science and Technology (R31-2008-000-10100-0), by the Korean Government under the Korea Science and Engineering Foundation (KOSEF) MOST Grant R01-2007-000-20377-0, and by the Center for Broadband Orthogonal Frequency Division Multi-plex Mobile Access, Pohang University of Science and Technology under the Information Technology Research Center Program of the Korean Ministry of Knowledge Economy, supervised by the Institute for Information Technology Advancement (IITA-2008-C1090-0801-0037).

REFERENCES

1. N. Ui and S. Sano, A 45% drain efficiency, -50 dBc ACLR GaN HEMT class-E amplifier with DPD for W-CDMA Base Station, IEEE MTT-S Int Microwave Symp Dig, San Francisco, CA (2006), 718–721.
2. S. Bensmida, O. Hammi, and F.M. Ghannouchi, High efficiency digitally linearized GaN based power amplifier for 3G applications, Proc 2008 IEEE Radio and Wireless Symp (2008), Atlanta, GA 419–422.
3. D.F. Kimball, J. Jeong, C. Hsia, P. Draxler, S. Lanfranco, W. Nagy, K. Linthicum, L.E. Larson, and P.M. Asbeck, High-efficiency envelope-tracking W-CDMA base-station amplifier using GaN HFETs, IEEE Trans Microwave Theory Technol 54 (2006), 3848–3856.
4. F. Wang, D.F. Kimball, J.D. Popp, A.H. Yang, D.Y. Lie, P.M. Asbeck, and L.E. Larson, An improved power-added efficiency 19-dBm hybrid envelope elimination and restoration power amplifier for 802.11g WLAN applications, IEEE Trans Microwave Theory Technol 54 (2006), 4086–4099.
5. J. Choi, J. Yim, J. Yang, J. Kim, J. Cha, D. Kang, D. Kim, and B. Kim, A delta-sigma-digitized polar RF transmitter, IEEE Trans Microwave Theory Technol 55 (2007), 2679–2690.
6. Y.Y. Woo, J. Kim, S. Hong, I. Kim, J. Moon, J. Yi, and B. Kim, A new adaptive digital predistortion technique employing feedback technique, IEEE MTT-S Int Microwave Symp Dig (2007), Honolulu, HI 1445–1448.
7. Y.Y. Woo, Y. Yang, and B. Kim, Analysis and experiments for high-efficiency class-F and inverse class-F power amplifiers, IEEE Trans Microwave Theory Technol 54 (2006), 1969–1974.
8. J. Vuolevi and T. Rahkonen, Distortion in RF Power Amplifiers. Artech House, Norwood, MA, 2003.
9. Connected simulation and test solutions using the advanced design system, Agilent Technol., Palo Alto, CA, Applicat. Note 1394, 2000.
10. J. Kim, Y.Y. Woo, J. Moon, and B. Kim, A new wideband adaptive digital predistortion technique employing feedback linearization, IEEE Trans Microwave Theory Technol 56 (2008), 385–392.

© 2009 Wiley Periodicals, Inc.

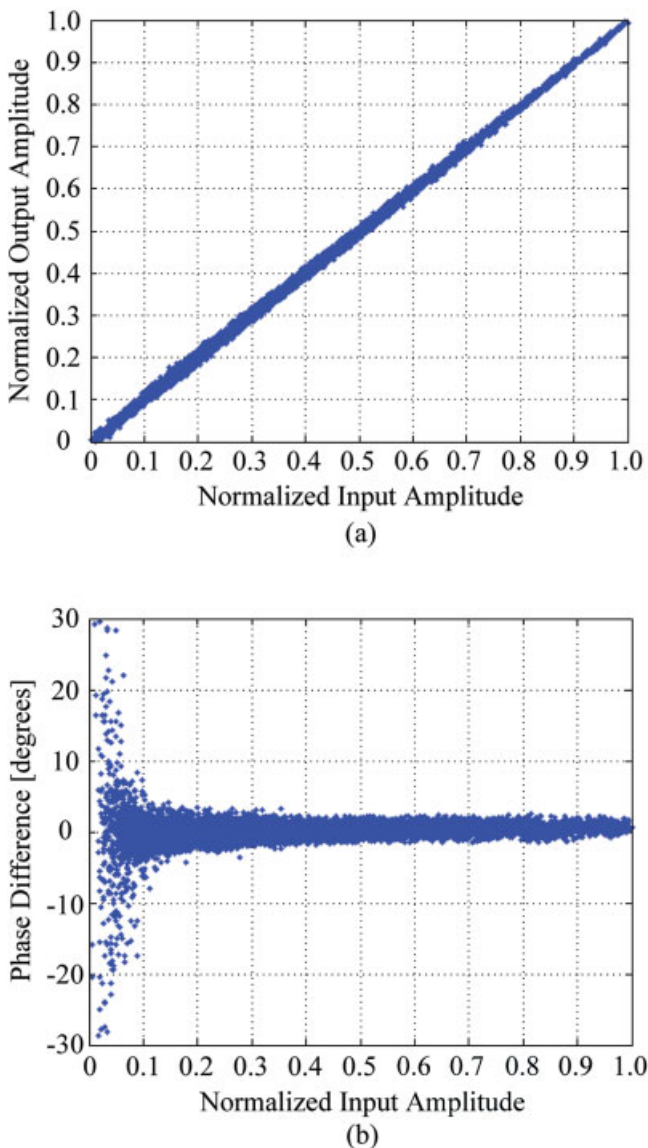


Figure 6 Measured (a) AM/AM and (b) AM/PM characteristics after the DFBDP linearization at an average output power of 32.3 dBm for WCDMA 3FA signal. [Color figure can be viewed in the online issue, which is available at www.interscience.wiley.com]